THE JOURNAL OF BIOLOGICAL CHEMISTRY VOL. 288, NO. 5, pp. 3620–3631, February 1, 2013

Assembly and Function of the Regulator of G protein Signaling 14 (RGS14)·H-Ras Signaling Complex in Live Cells Are Regulated by $G\alpha_{i1}$ and $G\alpha_i$-linked G Protein-coupled Receptors*

Received for publication, November 27, 2012, and in revised form, December 15, 2012 Published, JBC Papers in Press, December 17, 2012, DOI 10.1074/jbc.M112.440057

Christopher P. Vellano[‡], **Nicole E. Brown**[‡], **Joe B. Blumer**[§], **and John R. Hepler**[‡1]

From the [‡]*Department of Pharmacology, Emory University School of Medicine, Atlanta, Georgia 30322 and* [§]*Medical University of South Carolina, Department of Cell and Molecular Pharmacology and Experimental Therapeutics, Charleston, South Carolina 29425*

Background: RGS14 binds H-Ras to modulate its signaling.
Results: Inactive $G\alpha_{i1}$ and GPCRs regulate RGS14 interactions with activated H-Ras in live cells.
Conclusion: RGS14 simultaneously binds activated H-Ras and $G\alpha_{i1}$, forming a ternary complex that is regulated by GPCRs.
Significance: These findings highlight a possible mechanism for how RGS14 functions as a key regulator of hippocampal-based learning and memory.

Regulator of G protein signaling 14 (RGS14) is a multifunctional scaffolding protein that integrates heterotrimeric G protein and H-Ras signaling pathways. RGS14 possesses an RGS domain that binds active $G\alpha_{i/o}$-GTP subunits to promote GTP hydrolysis and a G protein regulatory (GPR) motif that selectively binds inactive $G\alpha_{i1/3}$-GDP subunits to form a stable heterodimer at cellular membranes. RGS14 also contains two tandem Ras/Rap binding domains (RBDs) that bind H-Ras. Here we show that RGS14 preferentially binds activated H-Ras-GTP in live cells to enhance H-Ras cellular actions and that this interaction is regulated by inactive $G\alpha_{i1}$-GDP and G protein-coupled receptors (GPCRs). Using bioluminescence resonance energy transfer (BRET) in live cells, we show that RGS14-Luciferase and active H-Ras(G/V)-Venus exhibit a robust BRET signal at the plasma membrane that is markedly enhanced in the presence of inactive $G\alpha_{i1}$-GDP but not active $G\alpha_{i1}$-GTP. Active H-Ras(G/V) interacts with a native RGS14·$G\alpha_{i1}$ complex in brain lysates, and co-expression of RGS14 and $G\alpha_{i1}$ in PC12 cells greatly enhances H-Ras(G/V) stimulatory effects on neurite outgrowth. Stimulation of the $G\alpha_i$-linked α_{2A}-adrenergic receptor induces a conformational change in the $G\alpha_{i1}$·RGS14·H-Ras(G/V) complex that may allow subsequent regulation of the complex by other binding partners. Together, these findings indicate that inactive $G\alpha_{i1}$-GDP enhances the affinity of RGS14 for H-Ras-GTP in live cells, resulting in a ternary signaling complex that is further regulated by GPCRs.

Canonical G protein signaling pathways include a G protein-coupled receptor (GPCR)[2] coupled to a heterotrimeric G protein ($G\alpha\beta\gamma$) that acts as a GTPase timing switch. Upon GPCR activation, the receptor acts as a guanine nucleotide exchange factor (GEF) and facilitates GDP release and subsequent GTP binding to the $G\alpha$ subunit that is followed by $G\beta\gamma$ dissociation/rearrangement from $G\alpha$-GTP. Free $G\beta\gamma$ and $G\alpha$-GTP are then able to engage downstream effectors and regulate signaling events (1, 2). Recent studies have examined the function of the regulators of G protein signaling (RGS) proteins in conventional G protein signaling, specifically how they act as GTPase accelerating proteins (GAPs) toward activated $G\alpha$ subunits. The conserved RGS domain binds and enhances the intrinsic rate of $G\alpha$ nucleotide hydrolysis, resulting in GPCR/G protein signal termination (3–5).

Regulator of G protein signaling 14 (RGS14) is a complex RGS protein grouped in the R12 subfamily of RGS proteins along with its closest relatives, RGS10 and RGS12 (3, 6). Predominately expressed in the hippocampus of brain (7, 8), RGS14 has been implicated in hippocampal-based learning, memory, and cognition (7, 9). The molecular mechanisms underlying these central nervous system (CNS) actions of RGS14, however, remain largely unknown. The highly unusual sequence and domain structure of RGS14 suggests it serves as a multifunctional scaffold that integrates G protein and H-Ras/MAPK signaling (10). In addition to the conserved RGS domain that confers GAP activity toward $G\alpha_{i/o}$ subunits (8, 11, 12), RGS14 also possesses two tandem Ras/Rap binding domains (RBDs) and a G protein regulatory (GPR) motif that binds selectively to inactive $G\alpha_{i1}$ and $G\alpha_{i3}$ subunits to form a stable complex at intracellular membranes (13–15). Recent work has shown that RGS14 participates in newly appreciated unconven-

* This work was supported, in whole or in part, by National Institutes of Health Grants R01NS049195 and R01NS037112 (to J. R. H.) and GM086510 (to J. B. B.) and by Microscopy Core of the Emory Neuroscience NINDS Core Facilities Grant P30NS055077. This work was also supported by a PhRMA Foundation Pre-doctoral Pharmacology/Toxicology Fellowship (to C. P. V).

[1] To whom correspondences should be addressed: Emory University School of Medicine, Dept. of Pharmacology, 1510 Clifton Rd., Rollins Research Center G206, Atlanta, GA 30322. Tel.: 404-727-3641; E-mail: jhepler@emory.edu.

[2] The abbreviations used are: GPCR, G protein-coupled receptor; GEF, guanine nucleotide exchange factor; RGS, regulators of G protein signaling; RGS14, regulator of G protein signaling 14; RBD, Ras/Rap binding domain; GPR, G protein regulatory motif; BRET, bioluminescence resonance energy transfer; Luc, luciferase; AR, adrenergic receptor.

tional G protein signaling networks, which involve G protein activation in the absence of GPCRs (16–23). Specifically, the RGS14·$G\alpha_{i1}$-GDP complex is regulated by the non-receptor GEF Ric-8A (24) both in the absence and presence of a coupled GPCR (25). This finding highlights a novel mechanism of action for an RGS protein, providing insight on how RGS14 may function within hippocampal neurons to regulate their signaling.

Although RGS14 may function within neurons by binding $G\alpha_{i1/3}$ and participating in unconventional G protein signaling pathways, evidence also suggests that RGS14 regulates MAPK signaling through binding H-Ras and Raf-1 via its RBDs (26). RGS14 binds directly to H-Ras via its first RBD (27), preferring to bind the activated form of H-Ras (26). By binding activated H-Ras, RGS14 inhibits PDGF-mediated ERK activation, an effect that is dependent on the presence of $G\alpha_{i1}$. When RGS14 is bound to $G\alpha_{i1}$, it can no longer bind Raf-1 and, therefore, can no longer regulate PDGF signaling (26). These results suggest that RGS14 may promote formation of a $G\alpha_{i1}$·RGS14·H-Ras ternary complex that serves as a molecular switch to regulate H-Ras/Raf-1 signaling on the one hand and $G\alpha_i$ signaling on the other. This would be similar to, and yet mechanistically distinct from GPCR cross-talk with growth factor stimulated Ras-mediated MAPK signaling (28–32). This idea of an RGS14 signaling switch mechanism has not yet been tested directly, and whether a GPCR may be involved in promoting this proposed switch mechanism is also unknown.

The goals of these studies were to investigate how RGS14/H-Ras interactions are regulated in live cells, specifically examining the effects of both active and inactive $G\alpha_i$ and GPCRs on this interaction. Using bioluminescence resonance energy transfer (BRET), we show that RGS14 binds preferentially to activated H-Ras in live cells and that this interaction and downstream cellular actions are greatly facilitated by complex formation with inactive $G\alpha_{i1}$ at the plasma membrane. In addition, activation of the $G\alpha_i$-linked α_{2A}-adrenergic receptor induces conformational changes within the $G\alpha_{i1}$·RGS14·H-Ras complex, supporting a functional link between GPCR/G protein coupling and H-Ras signaling. These findings indicate that GPCR activation may promote the switch mechanism of RGS14 and allow it to participate in both G protein and H-Ras signaling, which may ultimately underlie the function of RGS14 in regulating synaptic plasticity within hippocampal neurons (7).

EXPERIMENTAL PROCEDURES

Plasmids and Antibodies—The rat RGS14 cDNA used in this study (GenBank™ accession number U92279) was acquired as described (8). Wild-type (WT) and *GPR-null* rat RGS14-Luciferase (Luc) constructs were generated as previously described (25) using the phRLucN2 vector graciously provided by Dr. Michel Bouvier (University of Montreal). Venus-tagged H-Ras constructs were made from the parental H-Ras cDNA purchased from the UMR cDNA Resource Center (Rolla, MO). The $G\alpha_{i1}$-Q204L plasmid was also purchased from the UMR cDNA Resource Center. Venus-tagged wild-type H-Ras (H-Ras-WT-Venus) was generated by digesting the parental H-Ras-WT plasmid at EcoRI and SacII restriction sites and ligating the resulting product into Venus-C1 vector (graciously provided by Brandon Stauffer, Stephen Ikeda, and Steven Vogel, National Institutes of Health). Constitutively activated H-Ras(G/V)-Venus was generated by mutating the Gly-12 residue of H-Ras-WT-Venus to Val-12 using the QuikChange kit (Stratagene) and the following oligonucleotide primers: forward primer, 5′-AAT ATA AGC TGG TGG TGG TGG GCG CCG TCG GTG TGG GCA AGA GT-3′; reverse primer, 5′-ACT CTT GCC CAC ACC GAC GGC GCC CAC CAC CAC CAG CTT ATA TT-3′. The H-Ras C*AAX* box mutants (C186S mutation) were made using the QuikChange kit (Stratagene) and the following oligonucleotide primers: forward primer, 5′-GGC TGC ATG AGC TGC AAG TCT GTG CTC TCC-3′; reverse primer, 5′-GGA GAG CAC AGA CTT GCA GCT CAT GCA GCC-3′. The RGS14-R333L-Luc mutant was constructed using the QuikChange kit (Stratagene) and the following oligonucleotide primers: forward primer, 5′-GGC ATC TGT GAG AAG CTA GGC CTC TCT CTA CCT G-3′; reverse primer, 5′-CAG GTA GAG AGA GGC CTA GCT TCT CAC AGA TGC C-3′. Rat $G\alpha_{i1}$-EYFP ($G\alpha_{i1}$-YFP) in pcDNA3.1 was generated by Dr. Scott Gibson (University of Texas Southwestern) (33). α_{2A}-adrenergic receptor (α_{2A}-AR)-Venus and β_2-adrenergic receptor (β_2-AR)-Venus plasmids were generated as described and provided by Dr. Michel Bouvier (University of Montreal) (34, 35). Anti-sera used include Alexa 546 goat anti-rabbit secondary IgG (Invitrogen), Alexa 633 goat anti-mouse secondary IgG (Invitrogen), peroxidase-conjugated goat anti-mouse IgG (Rockland Immunochemicals, Inc.), peroxidase-conjugated goat anti-rabbit IgG (Bio-Rad), anti-$G\alpha_{i1}$ (Santa Cruz Biotechnologies, Inc.), anti-H-Ras (Abcam), anti-FLAG (Sigma), and anti-RGS14 (Antibodies, Inc.) antibodies.

Cell Culture and Transfection—HEK293 cells were maintained in Dulbecco's minimal essential medium (without phenol red) containing 10% fetal bovine serum (5% after transfection), 2 mM glutamine, 100 units/ml penicillin, and 100 mg/ml streptomycin. PC12 cells were maintained in Dulbecco's modified Eagle's medium supplemented with 5% fetal bovine serum (2.5% after transfection), 10% horse serum (5% after transfection), 100 units/ml penicillin, and 100 mg/ml streptomycin. Cells were incubated at 37 °C with 5% CO_2 in a humidified environment. Transfections were performed using previously described protocols with polyethyleneimine (Polysciences, Inc.) (36).

BRET in Live Cells—BRET experiments were performed as previously described (36, 37). Briefly, HEK293 cells were transiently transfected with BRET donor and acceptor plasmids using polyethyleneimine. Twenty-four to 48 hours after transfection, the culture medium was removed, and cells were harvested with Tyrode solution (140 mM NaCl, 5 mM KCl, 1 mM $MgCl_2$, 1 mM $CaCl_2$, 0.37 mM NaH_2PO_4, 24 mM $NaHCO_3$, 10 mM HEPES, and 0.1% glucose (w/v), pH 7.4). Cells were seeded in triplicate into gray 96-well OptiPlates (PerkinElmer Life Sciences) with each well containing 1×10^5 cells. The acceptor (YFP/Venus-tagged) protein expression levels were monitored by measuring total fluorescence using the TriStar LB 941 plate reader (Berthold Technologies) with excitation and emission filters at 485 and 535 nm, respectively. After fluorescence measurement, coelenterazine H (Nanolight Technology; 5 μM final concentration) was added, and luminescence was detected by

the TriStar LB 941 plate reader in the 480 ± 20- and 530 ± 20-nm ranges for donor (Luc) and acceptor (YFP/Venus), respectively. Samples of cells overexpressing α_{2A}-AR or β_2-AR were treated with either vehicle (Tyrode solution) or a final concentration of 10 μM UK14304 (Sigma) or 100 μM isoproterenol (Sigma), respectively, before the addition of coelenterazine. BRET signals were obtained by calculating the ratio of the light intensity emitted by the YFP/Venus divided by the light intensity emitted by Luc. Net BRET values were derived from subtracting the background BRET signal detected from the expression of the donor fusion protein (Luc) alone. All data were collected with MikroWin 2000 software and analyzed using Graphpad Prism and Microsoft Excel. Statistical analysis was performed using Student's *t* test, and immunoblots were performed as described previously (38).

Immunoprecipitation of RGS14 from Mouse Brain—HEK293 cells were transiently transfected with H-Ras(G/V). Eighteen hours post-transfection, cells were lysed in buffer containing 50 mM Tris-HCl, pH 8.0, 150 mM NaCl, 1 mM EGTA, 1 mM EDTA, 2 mM dithiothreitol, 5 mM $MgCl_2$, phosphatase inhibitor mixture (Sigma), protease inhibitor mixture (Roche Applied Science), and 1% Nonidet P-40. In parallel, two brains from C57BL6 wild-type mice were isolated and homogenized by a Dounce tissue grinder in the same lysis buffer stated above. Both cell and brain lysates were incubated on a 4 °C rotator for 1 h and then cleared by centrifugation at 100,000 × *g* for 30 min at 4 °C. Lysates were precleared by incubating with 50 μg of protein G-sepharose resin for 1 h on a 4 °C rotator. After preclearing, lysates were incubated in the absence or presence of a 1:50 dilution of anti-RGS14 antibody (Antibodies, Inc.) on a 4 °C rotator overnight. Next, 50 μg of BSA-preblocked protein G-sepharose resin was added to each sample. Samples were then rotated at 4 °C for 1.5 h. Resin was washed with ice-cold TBS four times, and proteins were eluted by the addition of Laemmli sample buffer and subsequent boiling for 5 min. Samples were resolved by SDS-PAGE, transferred to nitrocellulose membranes, and blotted with anti-RGS14, anti-Gα_{i1}, and anti-H-Ras antibodies followed by appropriate secondary antibodies. Proteins were detected by enhanced chemiluminescence.

Immunofluorescence and Confocal Imaging—Transfected HEK293 or PC12 cells were fixed at room temperature for 15 min in buffer containing 3.7% paraformaldehyde diluted in PBS. Cells were washed in PBS and incubated for 8 min with 0.4% Triton X-100 diluted in PBS. Cells were then blocked for 1 h at room temperature in PBS containing 10% goat serum and 3% BSA. Next, cells were incubated in this same buffer with a 1:1000 dilution of rabbit anti-FLAG and/or 1:300 dilution of mouse anti-Gα_{i1} antibodies at 37 °C for 1.5 h. Cells were washed with PBS (3×) and incubated with 1:300 dilutions of Alexa 546 goat anti-rabbit and Alexa 633 goat anti-mouse secondary antibodies at 37 °C for 1 h. Cells were washed with PBS again (3×) and mounted with ProLong Gold Antifade Reagent (Invitrogen). Confocal images were taken using a 63× oil immersion objective from an LSM510 laser scanning microscope with AxioObserver Stand (Zeiss). Images were processed using the ZEN 2009 Light Edition software and Adobe Photoshop 7.0 (Adobe Systems). Measurement and quantification of RGS14, Gα_{i1}, and H-Ras subcellular co-localization within cells was measured and plotted as relative fluorescence intensity using ImageJ software and analysis.

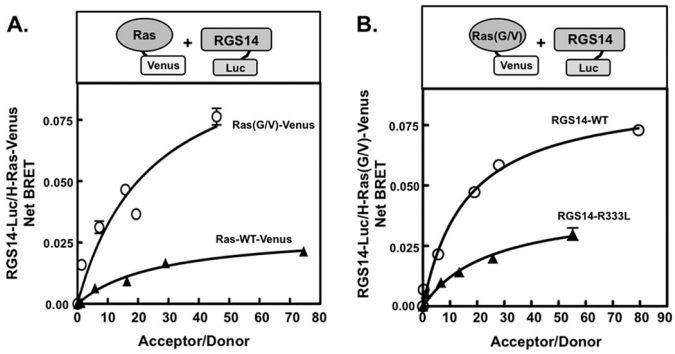

FIGURE 1. **RGS14 selectively interacts with activated H-Ras in live cells via the first RBD.** *A*, *top*, the diagram shows the RGS14-Luc/H-Ras-Venus BRET pair used for experimentation. *Bottom*, HEK cells were transfected with 5 ng of RGS14-Luc plasmid alone or in combination with 10, 50, 100, 250, or 500 ng of either H-Ras-WT-Venus or H-Ras(G/V)-Venus plasmid. BRET signals were measured, and net BRET was calculated as described under "Experimental Procedures." *B*, *Top*, the diagram shows the RGS14-Luc/H-Ras(G/V)-Venus BRET pair used for experimentation. *Bottom*, HEK cells were transfected with 5 ng of WT RGS14-Luc or RGS14-R333L-Luc plasmid alone or in combination with 10, 50, 100, 250, or 500 ng of H-Ras(G/V)-Venus plasmid. BRET signals were measured, and net BRET was calculated as in *A*. All data are expressed as the mean of three separate experiments, each with triplicate determinations.

Neurite Analysis of PC12 Cells—Twenty-four hours after transfection, cells were serum-starved overnight. Twenty-four hours later, cells were subjected to immunofluorescence and confocal imaging. Neurites were then counted and analyzed. Scored neurites were identified as cell protrusions having lengths of at least one cell body. In addition to the number of neurites, the percentage of cells with neurites at least two times longer than one cell body was also determined. Only cells confirmed to express all proteins of interest were analyzed. Statistical analysis was performed using one-way analysis of variance with Tukey's post-hoc test.

RESULTS

RGS14 Preferentially Interacts with Activated H-Ras via the First RBD—Because RGS14 has been shown to bind H-Ras both *in vitro* (27) and in cells through co-immunoprecipitation (26), we sought to quantitatively measure this interaction in live cells using BRET analysis. We first measured the magnitude and selectivity of a BRET signal between RGS14-Luc and either H-Ras-WT-Venus or constitutively activated H-Ras(G12V)-Venus (referred to as H-Ras(G/V)-Venus) (Fig. 1*A*). Transfection of HEK cells with increasing amounts of Venus-tagged H-Ras plasmids and a fixed amount (5 ng) of RGS14-Luc plasmid showed a robust BRET signal in the presence of H-Ras(G/V)-Venus, whereas an approximate 3-fold decrease in the maximal signal ($BRET_{max}$) was observed in the presence of H-Ras-WT-Venus (Fig. 1*A*). To determine the specificity of this interaction, H-Ras(G/V) was co-expressed with either WT RGS14 or the R333L mutant of RGS14 (Fig. 1*B*), which is reported not to bind H-Ras(G/V) in cell lysates (26). As in Fig. 1*A*, there was a strong BRET signal between RGS14-WT and H-Ras(G/V). This signal was reduced nearly 3-fold in the presence of RGS14-R333L but was not completely eliminated, consistent with our observation that this mutant retains a limited

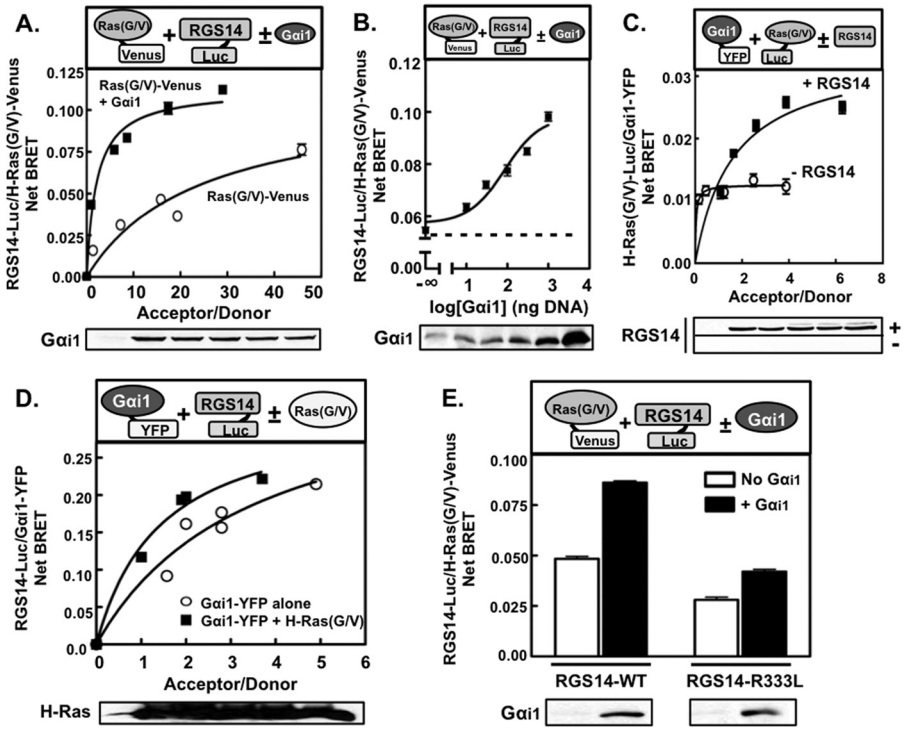

FIGURE 2. **RGS14 interactions with activated H-Ras in live cells are facilitated by Gα_{i1}.** *A*, *top*, the diagram shows the RGS14-Luc/H-Ras(G/V)-Venus BRET pair used for experimentation. *Bottom*, HEK cells were transfected with 5 ng of RGS14-Luc plasmid and either 0, 10, 50, 100, 250, or 500 ng of H-Ras(G/V)-Venus plasmid in the absence or presence of 750 ng of untagged Gα_{i1} plasmid. BRET signals were measured, and net BRET was calculated as described under "Experimental Procedures." *Bottom panel*, a representative immunoblot of Gα_{i1} expression is shown. Data are expressed as the mean of three separate experiments, each with triplicate determinations. *B*, *top*, the diagram shows the RGS14-Luc/H-Ras(G/V)-Venus BRET pair used for experimentation. *Bottom*, HEK cells were transfected with 5 ng of RGS14-Luc and 500 ng H-Ras(G/V)-Venus plasmids in combination with either 0, 10, 30, 100, 300, or 1000 ng of untagged Gα_{i1} plasmid. Net BRET signals were measured and calculated as in *A*. *Bottom panel*, shown is a representative immunoblot of Gα_{i1} expression. Data are expressed as the mean of three separate experiments, each with six determinations. *C*, *top*, the diagram shows the H-Ras(G/V)-Luc/Gα_{i1}-YFP BRET pair used for experimentation. *Bottom*, HEK cells were transfected with 5 ng of H-Ras(G/V)-Luc and either 0, 50, 100, 250, 500, or 750 ng of Gα_{i1}-YFP plasmid in the absence or presence of 750 ng of untagged FLAG-RGS14. Net BRET signals were measured and calculated as in *A*. *Bottom panel*, shown is a representative immunoblot of RGS14 expression in both the −RGS14 (−) and +RGS14 (+) conditions. Data are expressed as the mean of three separate experiments, each with six determinations. *D*, *top*, the diagram show the RGS14-Luc/Gα_{i1}-YFP BRET pair used for experimentation. *Bottom*, HEK cells were transfected with 5 ng of RGS14-Luc and either 0, 10, 50, 100, 250, or 500 ng of Gα_{i1}-YFP plasmid in the absence or presence of 750 ng of untagged H-Ras(G/V) plasmid. BRET signals were measured, and net BRET was calculated as in *A*. *Bottom panel*, shown is a representative immunoblot of H-Ras(G/V) expression. Data are expressed as the mean of two separate experiments, each with triplicate determinations. *E*, *top*, the diagram shows the RGS14-Luc/H-Ras(G/V)-Venus BRET pair used for experimentation. *Bottom*, HEK cells were transfected with 5 ng of WT or R333L RGS14-Luc plasmid and 500 ng of H-Ras(G/V)-Venus plasmid in the absence or presence of 750 ng of untagged Gα_{i1} plasmid. BRET signals were measured, and net BRET was calculated as in *A*. *Bottom panel*, shown is a representative immunoblot of Gα_{i1} expression. All data are expressed as the mean of three separate experiments, each with triplicate determinations.

capacity (albeit greatly reduced) to bind H-Ras in co-immunoprecipitation studies from these cells.[3] Furthermore, the observed large acceptor/donor ratio (H-Ras(G/V) to RGS14) that was required to generate these BRET signals indicates that this interaction is relatively weak, suggesting the requirement for other cellular binding partners and/or modifications that may optimize RGS14/H-Ras(G/V) interactions in cells.

Inactive Gα_{i1} Facilitates RGS14 Interactions with Activated H-Ras—Because our previous work suggests that RGS14 acts as a molecular switch for regulating MAPK and G protein signaling (26), we next tested the effects of Gα_{i1} on RGS14/H-Ras(G/V) BRET signals. The BRET signal between RGS14-Luc and increasing amounts of H-Ras(G/V)-Venus was measured in the absence or presence of Gα_{i1} (Fig. 2*A*). The observed RGS14/H-Ras(G/V) BRET signal (BRET$_{max}$) increased slightly in the presence of overexpressed Gα_{i1}, whereas the BRET$_{50}$ was significantly reduced (acceptor/donor ratio of 2 ± 0.732 *versus* 24 ± 4.8; $p < 0.05$) (Fig. 2*A*), indicating Gα_{i1}-mediated regulation of this complex. This effect was concentration-dependent, as increasing amounts of Gα_{i1} enhanced RGS14/H-Ras(G/V) BRET signals (Fig. 2*B*). Little detectable BRET signal was observed between membrane associated Gα_{i1}-YFP and H-Ras(G/V)-Luc (Fig. 2*C*). However, BRET activity between these two proteins was readily observed upon the addition of untagged RGS14 (Fig. 2*C*), strongly supporting the idea that RGS14 promotes assembly of a Gα_{i1}·RGS14·H-Ras ternary complex. This BRET signal was comparatively small, as would be expected because Gα_{i1}-YFP and H-Ras(G/V)-Luc are physically separated by RGS14. To test whether Gα_{i1} remained bound to RGS14 in the presence of H-Ras(G/V), the BRET signals between RGS14-Luc and Gα_{i1}-YFP were measured in the absence or presence of untagged H-Ras(G/V) (Fig. 2*D*). The BRET signals between RGS14 and Gα_{i1} remained relatively unchanged in the presence of H-Ras(G/V), suggesting that binding of Gα_{i1} and H-Ras are not mutually exclusive and further supporting the data from Fig. 2*C* that RGS14 may form a trimeric complex with Gα_i and H-Ras. We note that the YFP tag did not alter the function of Gα_{i1}, as insertion of the YFP tag

[3] F. J. Shu and J. R. Hepler, unpublished data.

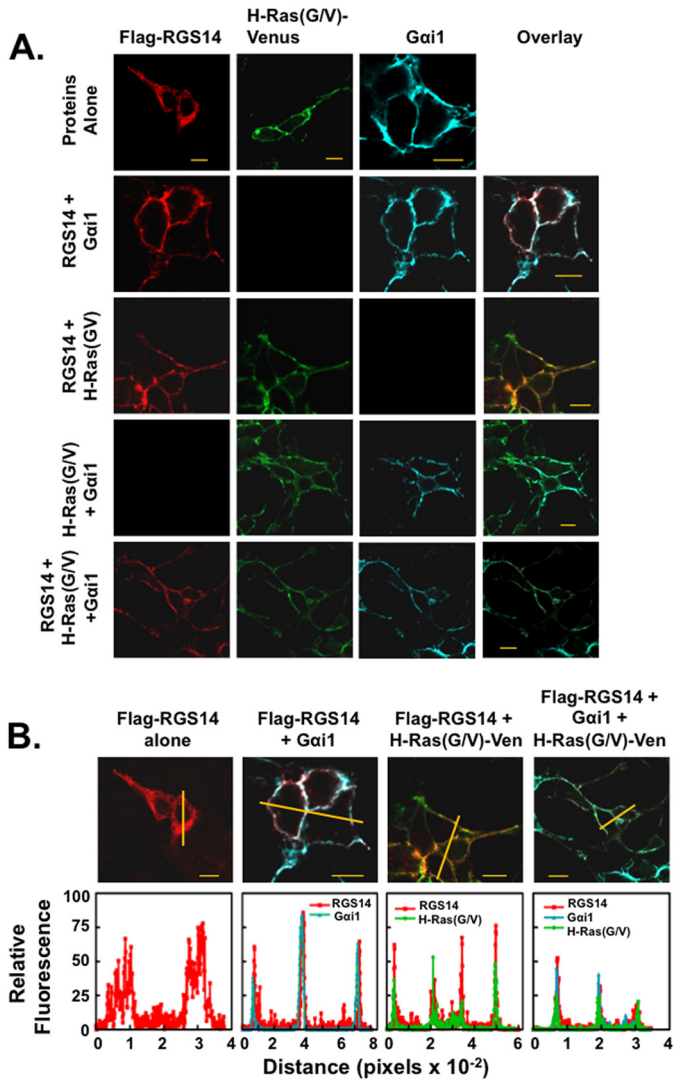

FIGURE 3. **RGS14 co-localizes with both Gα_{i1} and activated H-Ras at the plasma membrane.** *A*, FLAG-RGS14, Gα_{i1}, and H-Ras(G/V)-Venus were transfected into HEK cells alone and in combination. Cells were fixed, subjected to immunofluorescence, and analyzed using confocal microscopy as described under "Experimental Procedures." Images are representative of cells observed in three separate experiments. *B*, diagrams are shown illustrating quantification of either RGS14 localization alone, the RGS14-Gα_{i1} co-localization, the RGS14-H-Ras(G/V) co-localization, or the RGS14-H-Ras(G/V)-Gα_{i1} co-localization from Fig. 3. The relative fluorescence levels of FLAG-RGS14, H-Ras(G/V)-Venus, and Gα_{i1}-EE were measured (from *left to right* or *bottom to top*) across cross-sections (depicted by the *large orange line*) of the cell(s). The merged images are shown. The relative fluorescence was measured and analyzed using the ImageJ software program. *Scale bars* represent 10 μm.

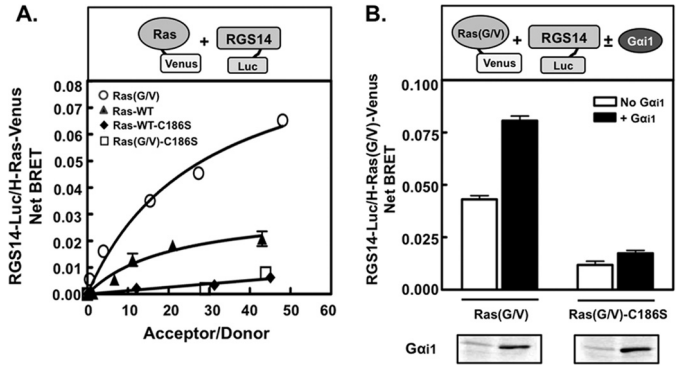

FIGURE 4. **RGS14/H-Ras(G/V) interactions depend on H-Ras(G/V) membrane localization.** *A*, *top*, the diagram shows the RGS14-Luc/H-Ras-Venus BRET pair used for experimentation. *Bottom*, HEK cells were transfected with 5 ng of RGS14-Luc plasmid and either 0, 10, 50, 100, 250, or 500 ng of either Venus-tagged H-Ras(G/V), WT H-Ras, H-Ras(G/V)-C186S, or H-Ras-WT-C186S plasmid. BRET signals were measured, and net BRET was calculated as described under "Experimental Procedures." *B*, *top*, the diagram shows the RGS14-Luc/H-Ras(G/V)-Venus BRET pair used for experimentation. *Bottom*, HEK cells were transfected with 5 ng of RGS14-Luc and 500 ng of either H-Ras(G/V)-Venus or H-Ras(G/V)-C186S-Venus plasmid in the presence or absence of 750 ng of untagged Gα_{i1} plasmid. BRET signals were measured, and net BRET was calculated as in *A*. *Bottom panel*, shown is a representative immunoblot of Gα_{i1} expression. All data are expressed as the mean of three separate experiments, each with triplicate determinations.

into the loop joining the αB and αC helices (33, 39, 40) retained nucleotide binding and hydrolysis properties similar to wild-type Gα_{i1} (33).

Supporting these BRET results, we observed that RGS14 translocated from the cytosol to the plasma membrane in the presence of either H-Ras(G/V), Gα_{i1}, or both (Fig. 3). When expressed alone in cells, RGS14 localized within the cytosol, whereas both Gα_{i1} and H-Ras(G/V) localized at the plasma membrane. However, when RGS14 was co-expressed with either Gα_{i1}, H-Ras(G/V), or both, RGS14 translocated to the plasma membrane and co-localized with Gα_{i1} and/or H-Ras(G/V). Given that there was little observable BRET signal between Gα_{i1} and H-Ras(G/V) (Fig. 2*C*) despite both being at the plasma membrane (Fig. 3), these findings suggest that RGS14 promotes formation of a heterotrimeric complex with both Gα_{i1} and activated H-Ras(G/V) at the plasma membrane.

Gα$_{i1}$-facilitated Interactions between RGS14 and Activated H-Ras Depend on the Gα$_{i1}$ Activation State and Plasma Membrane Localization of H-Ras—Because Gα_{i1} enhanced RGS14/H-Ras(G/V) BRET signals (Fig. 2, *A* and *B*) and the R333L mutation in RGS14 decreased these signals (Fig. 1*B*), we next determined the effects of Gα_{i1} expression on the BRET signals between H-Ras(G/V) and the RGS14-R333L mutant. In the presence of WT RGS14, the BRET signal between RGS14 and H-Ras(G/V) was enhanced by co-expressed Gα_{i1} (Fig. 2*E*). The RGS14-R333L mutant exhibited a 50% reduction in BRET signal with H-Ras(G/V) compared with RGS14-WT; however, this signal was still enhanced in the presence of co-expressed Gα_{i1} (Fig. 2*E*). The presence of Gα_{i1} induced an approximate 80% increase in RGS14/H-Ras(G/V) BRET signals in the presence of RGS14-WT as compared with only a 35% increase in the presence of RGS14-R333L. These findings illustrate the specificity of this Gα_{i1}-mediated effect. The observed BRET signal between RGS14-R333L and H-Ras(G/V) (Figs. 1*B* and 2*E*) likely reflects residual specific H-Ras binding to RGS14 as the R333L mutation fails to completely abolish H-Ras(G/V) binding.[3]

All of our data thus far suggest that H-Ras only interacts with RGS14 at the plasma membrane. To test this idea, the C186S mutation within the *CAAX* boxes of both wild-type H-Ras and H-Ras(G/V) was generated to prevent membrane localization (41–43). Specifically, this mutation prohibits the addition of lipid modifications that target H-Ras to the plasma membrane. The observed BRET signals between RGS14 and both H-Ras-WT and H-Ras(G/V) were almost completely ablated in the presence of the C186S H-Ras mutants (Fig. 4). Even the co-expression of Gα_{i1} could not overcome the loss of BRET

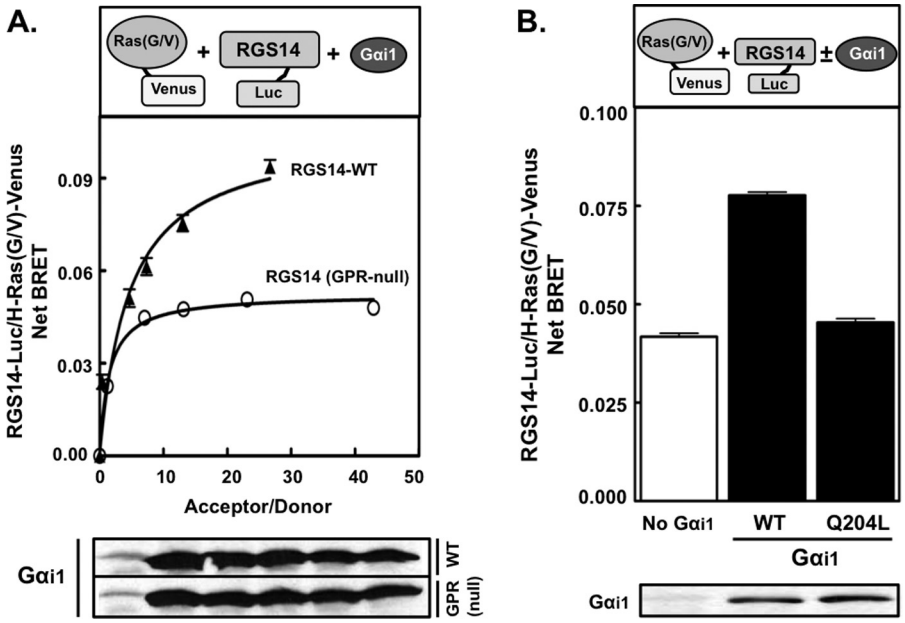

FIGURE 5. **RGS14/H-Ras(G/V) interactions depend on the Gα_{i1} activation state.** *A*, *top*, the diagram shows the RGS14-Luc/H-Ras(G/V)-Venus BRET pair used for experimentation. *Bottom*, HEK cells were transfected with 5 ng of WT or *GPR-null* RGS14-Luc plasmid and either 0, 10, 50, 100, 250, or 500 ng of H-Ras(G/V)-Venus plasmid in the presence of 750 ng of untagged Gα_{i1} plasmid. BRET signals were measured, and net BRET was calculated as described under "Experimental Procedures." *Bottom panel*, shown is a representative immunoblot of Gα_{i1} expression. *B*, *top*, the diagram shows the RGS14-Luc/H-Ras(G/V)-Venus BRET pair used for experimentation. *Bottom*, HEK cells were transfected with 5 ng of RGS14-Luc and 500 ng of H-Ras(G/V)-Venus plasmid in the presence of 750 ng of untagged WT or constitutively active (Q204L) Gα_{i1} plasmid. BRET signals were measured, and net BRET was calculated as in *A*. *Bottom panel*, shown is a representative immunoblot of Gα_{i1} expression. All data are expressed as the mean of three separate experiments, each with triplicate determinations.

signal generated by the H-Ras-C186S mutants (Fig. 4*B*), indicating that RGS14/H-Ras interactions and all generated BRET signals are specific and dependent on plasma membrane localization of H-Ras.

To determine whether Gα_{i1}-mediated effects on RGS14/H-Ras(G/V) interactions were dependent on the Gα_{i1} activation state, the BRET signals were measured between H-Ras(G/V) and RGS14-Q515A/R516A (referred to as RGS14(*GPR-null*)), which cannot bind inactive Gα_{i1} (25, 44, 45) (Fig. 5*A*). The Gα_{i1}-facilitated BRET between H-Ras(G/V) and RGS14-WT was abolished in the presence of RGS14(*GPR-null*), indicating that Gα_{i1} effects on these BRET signals are dependent on binding to the GPR motif. The effects of mutating Gα_{i1} in the presence of H-Ras(G/V) and wild-type RGS14 were also examined (Fig. 5*B*). The BRET signals observed between RGS14 and H-Ras(G/V) were enhanced by wild-type Gα_{i1} (WT) but remained unchanged in the presence of constitutively active Gα_{i1}-Q204L (Fig. 5*B*), further supporting a role for inactive Gα_{i1} in regulating RGS14 interactions with H-Ras in live cells.

RGS14 Interactions with Activated H-Ras Are Regulated by the Gα$_i$-linked α$_{2A}$-Adrenergic Receptor—We previously reported that the α_{2A}-AR functionally associates with the Gα_{i1}·RGS14 complex (25). Therefore, we next examined whether GPCRs could influence the RGS14·H-Ras(G/V) complex. For these studies, the BRET signals between RGS14-Luc and H-Ras(G/V)-Venus were analyzed in the presence of both Gα_{i1} and GPCRs, specifically the Gα_i-linked α_{2A}-AR and the Gα_s-linked β_2-AR (Fig. 6). In the absence of α_{2A}-AR receptor agonist, RGS14/H-Ras(G/V) BRET signals were similar to those seen in the presence of Gα_{i1} only (Figs. 2*A* and 6*A*). However, these signals decreased by ~35% in the presence of the α_{2A}-AR agonist UK14304 (*UK*) (Fig. 6*A*). Even with this decrease in signal (BRET$_{max}$), the BRET$_{50}$ values remained the same (acceptor/donor ratio of ~3.1), suggesting that activation of the GPCR induced a conformational change within the RGS14·H-Ras(G/V) complex rather than a dissociation of the complex. To expand on this idea, BRET signals were measured between RGS14-Luc and the α_{2A}-AR-Venus either in the absence or presence of untagged Gα_{i1} and H-Ras(G/V) (Fig. 6*B*; *left panel*) to determine if H-Ras(G/V) could influence RGS14 proximity to the receptor. As previously observed (25), there was little detectable BRET signal generated between RGS14 and the α_{2A}-AR when these two proteins were co-expressed in cells in the absence of Gα_{i1}. The addition of H-Ras(G/V) alone had little effect on RGS14/α_{2A}-AR BRET signals regardless of the presence of receptor agonist. However, a 4-fold increase in the BRET signal was observed between the α_{2A}-AR and RGS14 in the presence of co-expressed Gα_{i1} alone (Fig. 6*B*), as previously observed (25). This signal was reduced by >50% in the presence of UK14304, as previously observed (25). These Gα_{i1} effects were partially blocked in the presence of untagged H-Ras(G/V). In the absence of agonist, H-Ras(G/V) inhibited the Gα_{i1}-mediated BRET signal between RGS14 and the α_{2A}-AR by ~30%. In addition, H-Ras(G/V) blocked the agonist-induced decrease in RGS14/α_{2A}-AR BRET signals that was observed in the presence of Gα_{i1} only. As a negative control, the Gα_s-linked β_2-AR failed to recruit the Gα_{i1}·RGS14 complex (Fig. 6*B*; *right panel*). Together, these results suggest that H-Ras(G/V) and the α_{2A}-AR regulate one another's association with RGS14 in a Gα_{i1}-dependent manner.

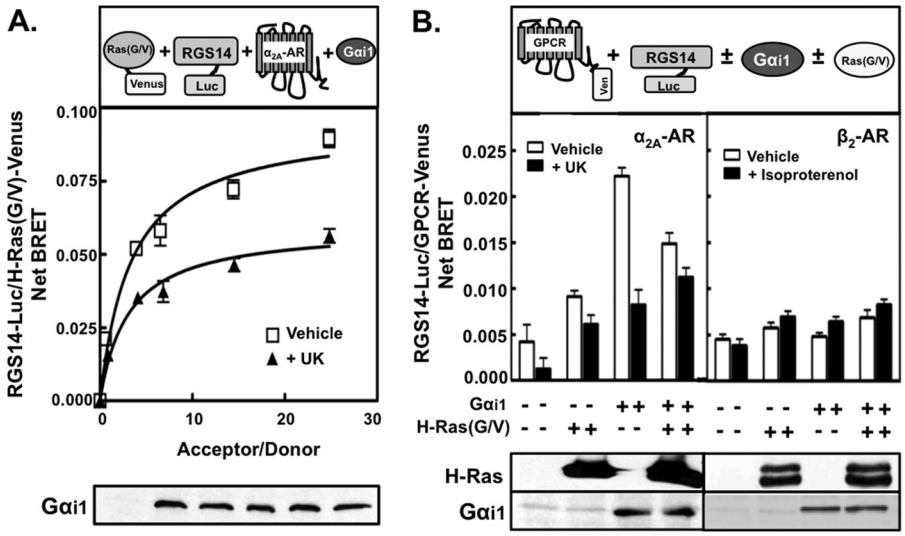

FIGURE 6. **The Gα$_i$-linked α$_{2A}$-AR associates with the Gα$_{i1}$·RGS14·H-Ras(G/V) complex.** *A*, *top*, the diagram shows the RGS14-Luc/H-Ras(G/V)-Venus BRET pair used for experimentation. *Bottom*, HEK cells were transfected with 5 ng of RGS14-Luc plasmid and either 0, 10, 50, 100, 250, or 500 ng of H-Ras(G/V)-Venus in the presence of 750 ng of untagged Gα$_{i1}$ and 500 ng of untagged α$_{2A}$-AR. Cells were treated with either vehicle or 10 μM UK14304 for 5 min. BRET signals were measured, and net BRET was calculated as described under "Experimental Procedures." *Bottom panel*, shown is a representative immunoblot of Gα$_{i1}$ expression. *B*, *top*, a diagram shows the RGS14-Luc/GPCR-Venus (*Ven*) BRET pair used for experimentation. *Bottom left*, HEK cells were transfected with 5 ng of RGS14-Luc and 500 ng of α$_{2A}$-AR-Venus plasmid in the presence or absence of 750 ng of untagged Gα$_{i1}$ and 500 ng of untagged H-Ras(G/V) plasmids. BRET signals were measured, and net BRET was calculated as in *A*. *Bottom right*, HEK cells were transfected with 5 ng of RGS14-Luc and 750 ng of β$_2$-AR-Venus plasmid in the presence or absence of 750 ng of untagged Gα$_{i1}$ and 250 ng of untagged H-Ras(G/V) plasmids. BRET signals were measured, and net BRET was calculated as in *A*, except stimulated cells were treated with 100 μM isoproterenol. *Bottom panel*, a representative immunoblot of Gα$_{i1}$ and H-Ras(G/V) expression is shown. All data are expressed as the mean of three separate experiments, with triplicate determinations for *A* and *B* (*left*) and four separate experiments with six determinations for *B* (*right*).

Native RGS14 Binds to Gα$_{i1}$ and Activated H-Ras in Mouse Brain—To highlight the physiological relevance of our BRET data showing that recombinant RGS14 binds to both exogenously expressed Gα$_{i1}$ and activated H-Ras in live cells (Figs. 1–6), we next examined whether native RGS14 could interact with native Gα$_{i1}$ and H-Ras in brain lysates. For these studies, we immunoprecipitated RGS14 out of mouse brain and measured whether native RGS14 bound to endogenous Gα$_{i1}$ and H-Ras (Fig. 7). We observed that native RGS14 bound to native Gα$_{i1}$ in brain lysates; however, it did not bind to native H-Ras. This is most likely due to the fact that native H-Ras in brain exists predominately in an inactive state. To ensure that H-Ras was activated, we incubated the brain lysates with HEK293 cell lysates overexpressing H-Ras(G/V). In combination with these HEK293 cell lysates, native RGS14 bound to both native Gα$_{i1}$ and the exogenous H-Ras(G/V), indicating formation of a heterotrimeric protein complex that may link G protein and H-Ras signaling pathways within brain.

RGS14 Promotes H-Ras-mediated Neurite Outgrowth in PC12 Cells—Because activated H-Ras has been shown to induce differentiation of and neurite outgrowth in PC12 cells (46) and because RGS14 has been linked to regulating growth factor-mediated neuritogenesis (47), we examined how RGS14 and Gα$_{i1}$ affected H-Ras-mediated PC12 cell differentiation and neurite outgrowth. Expression of H-Ras(G/V) alone in PC12 cells promoted greater neurite outgrowth compared with Venus vector only control (Fig. 8), inducing cells to acquire small, flat, thin cell bodies (Fig. 8*A*). Cells expressing both H-Ras(G/V) and Gα$_{i1}$ had smaller cell bodies and short neurites, whereas cells overexpressing H-Ras(G/V) and RGS14 had large, flat cell bodies and more neurites/cell compared with

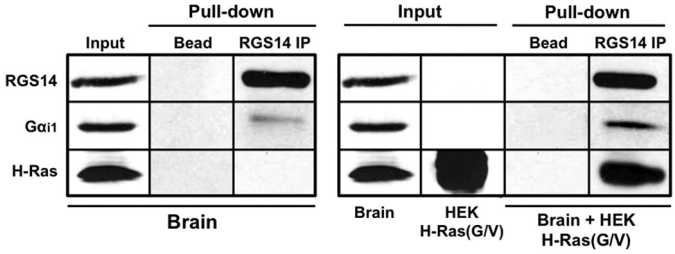

FIGURE 7. **Native RGS14 binds to native Gα$_{i1}$ and activated H-Ras in mouse brain.** Lysates from HEK cells transfected with 9 μg of H-Ras(G/V) plasmid were prepared in parallel with lysates derived from two mouse brains. Mouse brain lysates were either incubated alone or in combination with the HEK cell lysate either in the absence (*Bead*) or presence (*IP*) of anti-RGS14 antibody. Immunocomplexes were pulled down with protein G-Sepharose beads, and recovered proteins were subjected to SDS-PAGE and immunoblotting. This figure is representative of two separate experiments. Note: for clarity of presentation, images of the brain input in the *left panel* are equivalent to those of the brain input in the *right panel*.

cells overexpressing H-Ras(G/V) alone (Fig. 8, *A* and *B*). Cells overexpressing H-Ras(G/V), RGS14, and Gα$_{i1}$ together had very complex morphologies, with longer neurites and filopodia-like extensions (Fig. 8, *A* and *C*). These cells had both a greater number of neurites/cell and longer neurites, with lengths twice as long as one cell body (Fig. 8*C*). Of note, neither RGS14 alone nor Gα$_{i1}$ alone promoted differentiation and neurite outgrowth (Fig. 8*A*).

DISCUSSION

Recent evidence suggests that RGS14 switches between regulating G protein signaling and regulating H-Ras signaling (26); however, the mechanism(s) behind this molecular switch remains uncertain. Studies showing that the RGS14·Gα$_{i1}$ complex associates with GPCRs (25) and that GPCRs and Gα$_i$ are

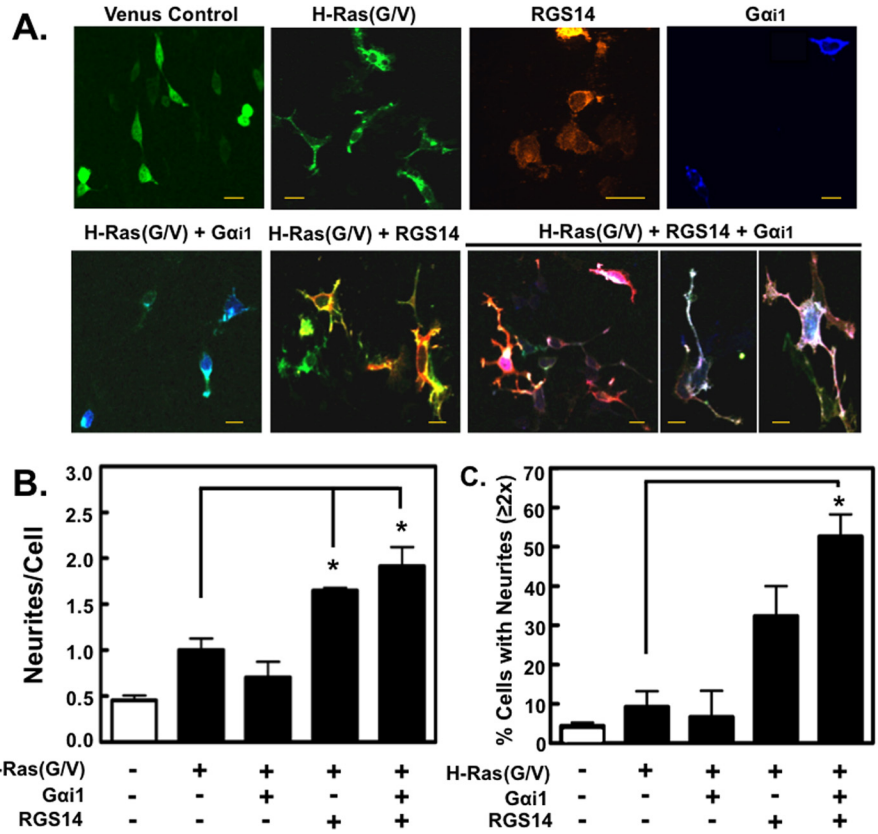

FIGURE 8. **RGS14 promotes H-Ras-mediated neurite outgrowth in PC12 cells.** *A*, PC12 cells were transfected with either Venus vector alone or combinations of H-Ras(G/V)-Venus, FLAG-RGS14, and Gα_{i1}. After 24 h, cells were serum-starved overnight. After another 24 h, cells were subjected to immunofluorescence and confocal imaging analysis. Images are representative of cells from three separate experiments. *Scale bars* represent 10 μm. Neurites with a length of at least one cell body were scored under each transfection condition (*B*). *C*, the percentage of cells with neurites exceeding 2× the length of one cell body (≥2×) was determined under each transfection condition. Statistical analysis was performed using one-way analysis of variance with Tukey's post-hoc test. *, $p < 0.05$ as compared with H-Ras(G/V) alone sample. Data are expressed as the mean neurite scores from three different experiments, with 10–70 cells assessed for each condition in each experiment. Only cells confirmed to express all proteins of interest were analyzed.

critical regulators of growth factor receptor signaling (28, 29, 48, 49) suggest that multiple non-canonical G protein signaling pathways may be involved in promoting this cross-talk. Our results with RGS14 support this idea and highlight a specific Gα_{i1}-directed mechanism underlying RGS14 interactions with H-Ras.

Overall, our findings here indicate the following: 1) RGS14 selectively interacts with activated H-Ras via the first RBD in live cells, 2) RGS14 interactions with activated H-Ras depend on the plasma membrane localization of H-Ras, 3) inactive Gα_{i1} greatly facilitates RGS14/H-Ras(G/V) interactions, 4) activation of the α_{2A}-AR receptor promotes rearrangement of the Gα_{i1}·RGS14·H-Ras(G/V) complex, 5) activated H-Ras regulates association/proximity of the Gα_{i1}·RGS14 complex with the α_{2A}-AR, 6) native RGS14 binds to Gα_{i1} and activated H-Ras in mouse brain lysates, and 7) RGS14 greatly facilitates H-Ras actions on neurite outgrowth in PC12 cells when in the presence of Gα_{i1}. Taken together, these findings suggest that RGS14 integrates both G protein signaling and H-Ras signaling through a unique mechanism that may include GPCRs to facilitate H-Ras cellular functions.

RGS14 Preferentially Interacts with the Activated Form of H-Ras in a Gα_{i1}-regulated Manner—Our BRET analysis indicates that RGS14 preferentially binds the active GTP-bound form of H-Ras in live cells and not the inactive GDP-bound form of the protein (Fig. 1*A*). Consistent with previous studies (26, 27), this interaction takes place via the first RBD of RGS14 (Fig. 1*B*). Surprisingly, this interaction was greatly facilitated by Gα_{i1} (Fig. 2, *A* and *B*), as the presence of overexpressed Gα_{i1} induced a marked decrease in the BRET$_{50}$, indicating that Gα_{i1} may either enhance the affinity of RGS14 for H-Ras or increase the number of RGS14·H-Ras(G/V) complexes. The fact that Gα_{i1} remained bound to RGS14 in the presence of H-Ras(G/V) (Fig. 2*D*) indicates that RGS14 can bind activated H-Ras and Gα_{i1} at the same time in live cells as has been postulated (26). This idea is most profoundly illustrated by our observation that RGS14 promotes the generation of BRET signals between Gα_{i1}-YFP and H-Ras(G/V)-Luc (Fig. 2*C*). Importantly, activated H-Ras and Gα_{i1} did not interact at the plasma membrane when co-expressed alone, indicating the absence of nonspecific bystander BRET between these two proteins.

These findings highlight mechanisms underlying the formation and regulation of the Gα_{i1}·RGS14·H-Ras(G/V) complex. Like other GPR proteins (50), RGS14 may form a clamshell-like structure that is regulated by its binding partners. Gα_{i1} binding to RGS14 may promote a conformational change in RGS14 that allows it to bind activated H-Ras more readily, thereby promoting a platform where RGS14 can switch from regulating G protein signaling to regulating H-Ras signaling. How or if Gα_{i1} ever dissociates from RGS14 upon H-Ras binding remains undeter-

mined; however, our results indicate that regardless of the temporal aspects of the regulation, RGS14 binds both Gα$_{i1}$ and activated H-Ras simultaneously.

A key component of this proposed switch mechanism is that only inactive Gα$_{i1}$ can facilitate H-Ras(G/V) binding to RGS14. It is possible that RGS14 can only assume a conformation favorable for binding active H-Ras when it is bound to Gα$_i$ via its GPR motif. The importance of the GPR motif in promoting RGS14 interactions with other non-Gα binding partners is also highlighted by our observation that the GPR motif is critical in promoting association between RGS14 and Gα$_{i1}$-linked GPCRs (Fig. 6 and Ref 25). Therefore, it is likely that Gα$_{i1}$ bound to the GPR motif may promote a stabilized and open conformation of RGS14 at the plasma membrane. This conformational switch may be a target for regulation by other signaling pathways because RGS14 is phosphorylated by PKA at Thr-494, a modification that enhances RGS14 affinity for Gα$_{i1}$ (51).

H-Ras Interactions with RGS14 Depend on H-Ras Membrane Localization—H-Ras(G/V) interacts with the Gα$_{i1}$-GDP·RGS14 complex via the first RBD of RGS14 because a mutant that strongly inhibits H-Ras binding to the RBD (R333L) (26) greatly reduces the H-Ras/RGS14 BRET signal (Figs. 1*B* and 2*E*). Our data with the H-Ras C*AAX* box mutants that are not lipid-modified (Fig. 4) clearly demonstrates that H-Ras only interacts with RGS14 when it is at the plasma membrane. Functionally, this is similar to H-Ras interactions with other effectors such as Raf-1, where H-Ras lipid modification and membrane association are essential for its capacity to activate Raf-1 (summarized in Ref. 52). Our findings indicate that Gα$_{i1}$ is necessary for recruiting RGS14 to the plasma membrane and anchoring it there (15, 24) and that this complex is what membrane-bound H-Ras recognizes. Both Gα$_{i1}$ and H-Ras are lipid-modified to anchor them to the membrane, whereas RGS14 is not,[4] suggesting that RGS14 can be recruited to different subcellular membranes depending on the presence/absence of membrane-bound binding partners. Indeed, recombinant RGS14 is reported to localize to centrosomes with Gα$_{i1}$ in non-neuronal cells (15, 53). When in complex with Gα$_{i1}$ at the plasma membrane, RGS14 may reside within specific lipid microdomains and serve to sequester active H-Ras away from its other downstream effectors and/or redirect H-Ras signaling to a different effector. At the same time, RGS14 when in complex with Gα$_{i1}$ and H-Ras may itself serve as a novel effector to recruit other (yet unknown) downstream signaling partners. Further studies are in progress to distinguish between these possibilities.

RGS14 Promotes H-Ras-mediated Neurite Outgrowth in PC12 Cells—To determine a possible functional effect of RGS14 and Gα$_{i1}$ on H-Ras signaling, we examined the role of both on regulating H-Ras-mediated neurite outgrowth in PC12 cells where RGS14 mRNA is reported to be expressed (47). H-Ras-induced cell differentiation is significantly enhanced in the presence of both RGS14 and Gα$_{i1}$, with cells exhibiting both a greater number and length of neurites (Fig. 8). Inactive Gα$_{i1}$ recruits RGS14 to the membrane, where the RGS14·Gα$_{i1}$ complex has a greater affinity for H-Ras (see Fig. 2*A*). Formation of this ternary protein complex may allow activated H-Ras and/or RGS14 to engage more efficiently with downstream effectors that promote changes in cytoskeleton filament length and organization that enhance neurite outgrowth. RGS14 may form a complex with Gα$_{i1}$ and activated H-Ras to mediate signaling through one or more cell surface receptors, although further studies are needed to confirm this idea. By binding Gα$_{i1}$ and/or switching to bind activated H-Ras in hippocampal neurons, RGS14 may play a significant role in postsynaptic signaling responsible for dendrite and spine remodeling.

Working Model for How RGS14 Integrates G Protein and H-Ras-mediated Signaling—Our findings here, when combined with our earlier findings (9, 25, 26), highlight a novel mechanism of action for RGS14 where it sits at the interface of both G protein and H-Ras signaling. One potential model to explain this mechanism is consistent with two cellular pools of RGS14·Gα$_{i1}$ complexes, as has been postulated (25). In this model one pool of RGS14·Gα$_{i1}$ complexes may be localized at the plasma membrane and functionally linked to GPCRs, as implied by the Gα$_{i1}$-dependent BRET signal observed between RGS14 and the α$_{2A}$-AR (Fig. 6; Ref. 25). This may involve direct coupling to a Gα$_{i1}$·RGS14 complex or merely close proximity as BRET does not distinguish between these two scenarios. The other pool of RGS14·Gα$_{i1}$ complexes may localize at the plasma membrane but not associate with GPCRs, allowing these complexes to bind other proteins such as activated H-Ras. This is supported by the decrease in Gα$_{i1}$-dependent RGS14/α$_{2A}$-AR BRET signals observed in the presence of untagged activated H-Ras (Fig. 6*B*). In the absence of overexpressed H-Ras(G/V), there may be an abundance of RGS14·Gα$_{i1}$ complexes that couple with the GPCR. When H-Ras(G/V) is introduced into cells, some of these RGS14·Gα$_{i1}$ complexes shift away from receptors and bind to activated H-Ras. We should note, however, that activated H-Ras only induces a modest decrease in the Gα$_{i1}$-dependent RGS14/α$_{2A}$-AR BRET signals, which suggests that binding of activated H-Ras to a putative GPCR·Gα$_{i1}$·RGS14 complex may only induce conformational rearrangement. In this case, activated H-Ras would not compete for RGS14 binding.

An attractive alternative model that is supported by the data presented here suggests that a preformed GPCR·Gα$_{i1}$·RGS14 complex can be regulated by activated H-Ras (see Fig. 9). Gα$_{i1}$ is bound to both the GPCR and RGS14, thereby bringing RGS14 in close proximity but not necessarily in direct contact with the receptor. In this model stimulation of a Ras-GEF promotes activation of H-Ras, which then localizes to the plasma membrane adjacent to the RGS14·Gα$_{i1}$ complex (Fig. 9; *steps 1* and *2*). Activation of H-Ras presents a high affinity substrate for the preformed RGS14·Gα$_{i1}$ complex, allowing RGS14 to bind H-Ras-GTP very tightly via its first RBD (Fig. 9; *steps 2* and *3*). Activation of the coupled GPCR induces a conformational change in RGS14 (see Fig. 6*A*), which alters the proximity of RGS14 with both the GPCR and activated H-Ras (Fig. 9; *step 4*). Because the non-receptor GEF Ric-8A has been shown to induce dissociation of the RGS14·Gα$_{i1}$ complex (24, 25), we propose that GPCR·Gα$_i$·RGS14 complex rearrangement after GPCR stimulation may allow such a non-receptor GEF to act on

[4] K. H. Pedone and J. R. Hepler, unpublished data.

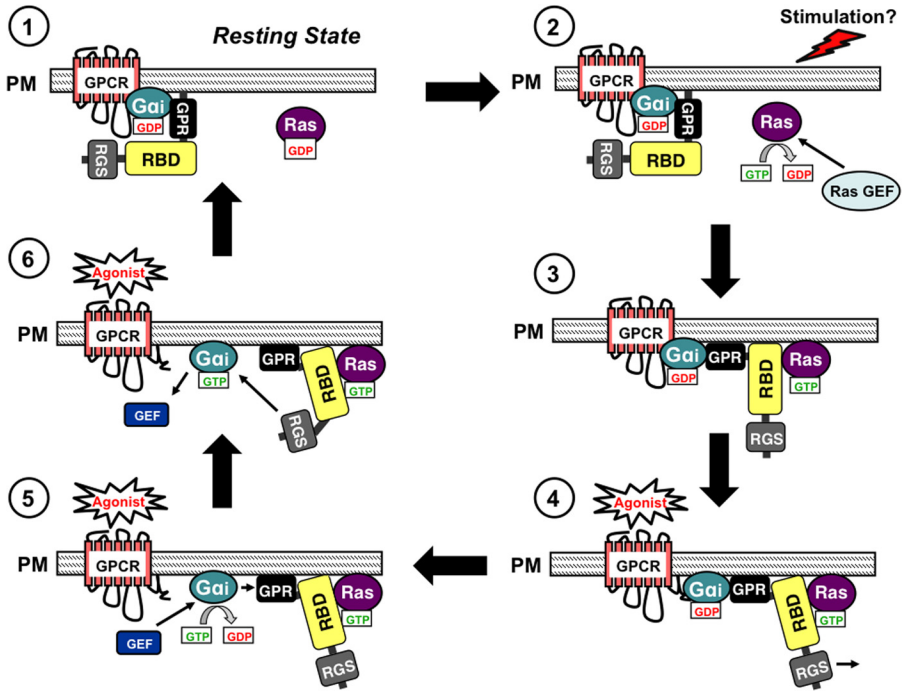

FIGURE 9. **Proposed working model for how RGS14 integrates G protein and Ras-mediated signaling.** The proposed model for RGS14 signaling proceeds clockwise from *top left* (*steps 1–6*). *1*, in the basal resting state of the cell, RGS14 exists in complex with inactive $G\alpha_i$-GDP via its GPR motif and with a GPCR at the plasma membrane (*PM*). *2*, any one of many possible stimulation events activates a Ras-GEF, which is then recruited to H-Ras-GDP and catalyzes nucleotide exchange to activate H-Ras. *3*, RGS14 now binds activated H-Ras-GTP to form a multiprotein complex consisting of the GPCR, $G\alpha_i$, RGS14, and H-Ras-GTP. *4*, GPCR stimulation induces a conformational change in RGS14 while still in complex with both $G\alpha_i$ and H-Ras-GTP. *5*, the $G\alpha_i$ released from the activated receptor is now a substrate for a non-receptor GEF to catalyze nucleotide exchange, which ultimately facilitates $G\alpha_i$ release from the RGS14·H-Ras-GTP complex. *6*, in some regulated fashion, the adjacent RGS domain of RGS14 recognizes the active $G\alpha_i$ to accelerate $G\alpha$-GTP hydrolysis, resulting in signal termination. The nearby GPR motif re-binds $G\alpha_i$-GDP after H-Ras dissociation, leading to reformation of the inactive RGS14·$G\alpha_i$-GDP complex and a return to the basal resting state (*1*).

the available $G\alpha_i$ (Fig. 9; *step 5*). In this case the GEF catalyzes nucleotide exchange to activate $G\alpha_{i1}$. The RGS domain of RGS14, being in close proximity, may then recognize and act as a GTPase-accelerating protein toward the activated $G\alpha_{i1}$ to restore $G\alpha_{i1}$-GDP (Fig. 9; *step 6*). The GPR motif would then rebind the now inactive $G\alpha_i$ to reform a GPCR·$G\alpha_{i1}$·RGS14 complex (Fig. 9; *step 1*). The workings of this model may take place within hippocampal neurons, with RGS14 serving to localize H-Ras to the correct place in the cell for interaction with an effector that promotes neurite outgrowth (Fig. 8) or dendrite/spine remodeling associated with synaptic plasticity (54). Taken together, this model highlights a potential mechanism for RGS14 involvement in GPCR cross-talk with H-Ras-mediated signaling.

Collectively, our findings show that RGS14 functions to integrate both G protein and Ras-mediated signaling. We showcase newly appreciated roles for RGS14 at the interface of G protein and H-Ras signaling pathways, in particular its capacity to act as a molecular switch between regulating these two pathways. The fact that native RGS14 binds to native $G\alpha_{i1}$ and H-Ras(G/V) in brain (Fig. 7) suggests that RGS14 may function as a switch to regulate both GPCR/G protein and H-Ras-mediated signaling in hippocampal neurons. Because H-Ras, $G\alpha_{i1}$, and the non-receptor GEF Ric-8A have been implicated in regulating similar hippocampal signaling pathways and functions (55–59), the molecular mechanisms we observe here may provide insight on how RGS14 functions physiologically within the brain to regulate synaptic plasticity and hippocampal-based learning, memory, and cognition (7, 9).

Acknowledgments—We thank Dr. Oskar Laur of the Custom Cloning Core Facility (Emory University School of Medicine) for generating H-Ras-Venus plasmids and Brandon Stauffer, Dr. Stephen Ikeda, and Dr. Steven Vogel (National Institutes of Health) for providing the Venus-C1 vector. We also thank Dr. Michel Bouvier (Universite de Montreal) for the α2A-AR-Venus, β2-AR-Venus, and the phRLucN vectors.

REFERENCES

1. Gilman, A. G. (1987) G proteins. Transducers of receptor-generated signals. *Annu. Rev. Biochem.* **56,** 615–649
2. Hamm, H. E. (1998) The many faces of G protein signaling. *J. Biol. Chem.* **273,** 669–672
3. Hollinger, S., and Hepler, J. R. (2002) Cellular regulation of RGS proteins. Modulators and integrators of G protein signaling. *Pharmacol. Rev.* **54,** 527–559
4. Ross, E. M., and Wilkie, T. M. (2000) GTPase-activating proteins for heterotrimeric G proteins. Regulators of G protein signaling (RGS) and RGS-like proteins. *Annu. Rev. Biochem.* **69,** 795–827
5. De Vries, L., Zheng, B., Fischer, T., Elenko, E., and Farquhar, M. G. (2000) The regulator of G protein signaling family. *Annu. Rev. Pharmacol. Toxicol.* **40,** 235–271
6. Kimple, A. J., Bosch, D. E., Giguère, P. M., and Siderovski, D. P. (2011) Regulators of G-protein signaling and their Gα substrates. Promises and challenges in their use as drug discovery targets. *Pharmacol. Rev.* **63,** 728–749

7. Lee, S. E., Simons, S. B., Heldt, S. A., Zhao, M., Schroeder, J. P., Vellano, C. P., Cowan, D. P., Ramineni, S., Yates, C. K., Feng, Y., Smith, Y., Sweatt, J. D., Weinshenker, D., Ressler, K. J., Dudek, S. M., and Hepler, J. R. (2010) RGS14 is a natural suppressor of both synaptic plasticity in CA2 neurons and hippocampal-based learning and memory. *Proc. Natl. Acad. Sci. U.S.A.* **107,** 16994–16998
8. Hollinger, S., Taylor, J. B., Goldman, E. H., and Hepler, J. R. (2001) RGS14 is a bifunctional regulator of G$\alpha_{i/o}$ activity that exists in multiple populations in brain. *J. Neurochem.* **79,** 941–949
9. Vellano, C. P., Lee, S. E., Dudek, S. M., and Hepler, J. R. (2011) RGS14 at the interface of hippocampal signaling and synaptic plasticity. *Trends Pharmacol. Sci.* **32,** 666–674
10. Snow, B. E., Antonio, L., Suggs, S., Gutstein, H. B., and Siderovski, D. P. (1997) Molecular cloning and expression analysis of rat Rgs12 and Rgs14. *Biochem. Biophys. Res. Commun.* **233,** 770–777
11. Cho, H., Kozasa, T., Takekoshi, K., De Gunzburg, J., and Kehrl, J. H. (2000) RGS14, a GTPase-activating protein for Giα, attenuates Giα- and G13α-mediated signaling pathways. *Mol. Pharmacol.* **58,** 569–576
12. Traver, S., Bidot, C., Spassky, N., Baltauss, T., De Tand, M. F., Thomas, J. L., Zalc, B., Janoueix-Lerosey, I., and Gunzburg, J. D. (2000) RGS14 is a novel Rap effector that preferentially regulates the GTPase activity of Gα_o. *Biochem. J.* **350,** 19–29
13. Kimple, R. J., De Vries, L., Tronchère, H., Behe, C. I., Morris, R. A., Gist Farquhar, M., and Siderovski, D. P. (2001) RGS12 and RGS14 GoLoco motifs are Gα_i interaction sites with guanine nucleotide dissociation inhibitor activity. *J. Biol. Chem.* **276,** 29275–29281
14. Mittal, V., and Linder, M. E. (2004) The RGS14 GoLoco domain discriminates among Gα_i isoforms. *J. Biol. Chem.* **279,** 46772–46778
15. Shu, F.-J., Ramineni, S., Amyot, W., and Hepler, J. R. (2007) Selective interactions between Giα1 and Giα3 and the GoLoco/GPR domain of RGS14 influence its dynamic subcellular localization. *Cell. Signal.* **19,** 163–176
16. Colombo, K., Grill, S. W., Kimple, R. J., Willard, F. S., Siderovski, D. P., and Gönczy, P. (2003) Translation of polarity cues into asymmetric spindle positioning in *Caenorhabditis elegans* embryos. *Science* **300,** 1957–1961
17. Groves, B., Gong, Q., Xu, Z., Huntsman, C., Nguyen, C., Li, D., and Ma, D. (2007) A specific role of AGS3 in the surface expression of plasma membrane proteins. *Proc. Natl. Acad. Sci. U.S.A.* **104,** 18103–18108
18. Hampoelz, B., and Knoblich, J. A. (2004) Heterotrimeric G proteins. New tricks for an old dog. *Cell* **119,** 453–456
19. Sans, N., Wang, P. Y., Du, Q., Petralia, R. S., Wang, Y.-X., Nakka, S., Blumer, J. B., Macara, I. G., and Wenthold, R. J. (2005) mPins modulates PSD-95 and SAP102 trafficking and influences NMDA receptor surface expression. *Nat. Cell Biol.* **7,** 1179–1190
20. Sato, M., Blumer, J. B., Simon, V., and Lanier, S. M. (2006) Accessory proteins for G proteins. Partners in signaling. *Annu. Rev. Pharmacol. Toxicol.* **46,** 151–187
21. Willard, F. S., Kimple, R. J., and Siderovski, D. P. (2004) Return of the GDI. The GoLoco motif in cell division. *Annu. Rev. Biochem.* **73,** 925–951
22. Schade, M. A., Reynolds, N. K., Dollins, C. M., and Miller, K. G. (2005) Mutations that rescue the paralysis of *C. elegans* ric-8 (Synembryn) mutants activate the Gα_s pathway and define a third major branch of the synaptic signaling network. *Genetics* **169,** 631–649
23. Hess, H. A., Röper, J.-C., Grill, S. W., and Koelle, M. R. (2004) RGS-7 completes a receptor-independent heterotrimeric G protein cycle to asymmetrically regulate mitotic spindle positioning in C. elegans. *Cell* **119,** 209–218
24. Vellano, C. P., Shu, F.-J., Ramineni, S., Yates, C. K., Tall, G. G., and Hepler, J. R. (2011) Activation of the regulator of G protein signaling 14-Gα_{i1}-GDP signaling complex is regulated by resistance to inhibitors of cholinesterase-8A. *Biochemistry* **50,** 752–762
25. Vellano, C. P., Maher, E. M., Hepler, J. R., and Blumer, J. B. (2011) G protein-coupled receptors and resistance to inhibitors of cholinesterase-8A (Ric-8A) both regulate the regulator of G protein signaling 14 (RGS14)·Gα_{i1} complex in live cells. *J. Biol. Chem.* **286,** 38659–38669
26. Shu, F.-J., Ramineni, S., and Hepler, J. R. (2010) RGS14 is a multifunctional scaffold that integrates G protein and Ras/Raf MAP kinase signalling pathways. *Cell. Signal.* **22,** 366–376
27. Kiel, C., Wohlgemuth, S., Rousseau, F., Schymkowitz, J., Ferkinghoff-Borg, J., Wittinghofer, F., and Serrano, L. (2005) Recognizing and defining true Ras binding domains II. *In silico* prediction based on homology modelling and energy calculations. *J. Mol. Biol.* **348,** 759–775
28. Alderton, F., Rakhit, S., Kong, K. C., Palmer, T., Sambi, B., Pyne, S., and Pyne, N. J. (2001) Tethering of the platelet-derived growth factor β receptor to G-protein-coupled receptors. *J. Biol. Chem.* **276,** 28578–28585
29. Conway, A. M., Rakhit, S., Pyne, S., and Pyne, N. J. (1999) Platelet-derived growth factor stimulation of the p42/p44 mitogen-activated protein kinase pathway in airway smooth muscle. Role of pertussis toxin-sensitive G-proteins, c-Src tyrosine kinases, and phosphoinositide 3-kinase. *Biochem. J.* **337,** 171–177
30. Daub, H., Weiss, F. U., Wallasch, C., and Ullrich, A. (1996) Role of transactivation of the EGF receptor in signalling by G-protein-coupled receptors. *Nature* **379,** 557–560
31. Fischer O. M., Hart, S., Gschwind A, and Ullrich A. (2003) EGFR signal transactivation in cancer cells. *Biochem. Soc. Trans.* **31,** 1203–1208
32. Prenzel, N., Zwick, E., Daub, H., Leserer, M., Abraham, R., Wallasch, C., and Ullrich, A. (1999) EGF receptor transactivation by G-protein-coupled receptors requires metalloproteinase cleavage of proHB-EGF. *Nature* **402,** 884–888
33. Gibson, S. K., and Gilman, A. G. (2006) Giα and Gβ subunits both define selectivity of G protein activation by α2-adrenergic receptors. *Proc. Natl. Acad. Sci. U.S.A.* **103,** 212–217
34. Duzic, E., Coupry, I., Downing, S., and Lanier, S. M. (1992) Factors determining the specificity of signal transduction by guanine nucleotide-binding protein-coupled receptors. I. Coupling of α2-adrenergic receptor subtypes to distinct G-proteins. *J. Biol. Chem.* **267,** 9844–9851
35. Galés, C., Van Durm, J. J., Schaak, S., Pontier, S., Percherancier, Y., Audet, M., Paris, H., and Bouvier, M. (2006) Probing the activation-promoted structural rearrangements in preassembled receptor-G protein complexes. *Nat. Struct. Mol. Biol.* **13,** 778–786
36. Oner, S. S., Maher, E. M., Breton, B., Bouvier, M., and Blumer, J. B. (2010) Receptor-regulated interaction of activator of G-protein signaling-4 and Gα_i. *J. Biol. Chem.* **285,** 20588–20594
37. Oner, S. S., An, N., Vural, A., Breton, B., Bouvier, M., Blumer, J. B., and Lanier, S. M. (2010) Regulation of the AGS3·Gα_i signaling complex by a seven-transmembrane span receptor. *J. Biol. Chem.* **285,** 33949–33958
38. Blumer, J. B., Chandler, L. J., and Lanier, S. M. (2002) Expression analysis and subcellular distribution of the two G-protein regulators AGS3 and LGN indicate distinct functionality. *J. Biol. Chem.* **277,** 15897–15903
39. Hein, P., Rochais, F., Hoffmann, C., Dorsch, S., Nikolaev, V. O., Engelhardt, S., Berlot, C. H., Lohse, M. J., and Bünemann, M. (2006) G$_s$ activation is time-limiting in initiating receptor-mediated signaling. *J. Biol. Chem.* **281,** 33345–33351
40. Hynes, T. R., Mervine, S. M., Yost, E. A., Sabo, J. L., and Berlot, C. H. (2004) Live cell imaging of G$_s$ and the β2-adrenergic receptor demonstrates that both αs and β1γ7 internalize upon stimulation and exhibit similar trafficking patterns that differ from that of the β2-adrenergic receptor. *J. Biol. Chem.* **279,** 44101–44112
41. Casey, P. J., Solski, P. A., Der, C. J., and Buss, J. E. (1989) p21ras is modified by a farnesyl isoprenoid. *Proc. Natl. Acad. Sci. U.S.A.* **86,** 8323–8327
42. Deschenes, R. J., Stimmel, J. B., Clarke, S., Stock, J., and Broach, J. R. (1989) RAS2 protein of *Saccharomyces cerevisiae* is methyl-esterified at its carboxyl terminus. *J. Biol. Chem.* **264,** 11865–11873
43. Schmidt, W. K., Tam, A., Fujimura-Kamada, K., and Michaelis, S. (1998) Endoplasmic reticulum membrane localization of Rce1p and Ste24p, yeast proteases involved in carboxyl-terminal C*AAX* protein processing and amino-terminal a-factor cleavage. *Proc. Natl. Acad. Sci. U.S.A.* **95,** 11175–11180
44. Khafizov, K. (2009) GoLoco motif proteins binding to Gα_{i1}. Insights from molecular simulations. *J. Mol. Model.* **15,** 1491–1499
45. Kimple, R. J., Kimple, M. E., Betts, L., Sondek, J., and Siderovski, D. P. (2002) Structural determinants for GoLoco-induced inhibition of nucleotide release by Gα subunits. *Nature* **416,** 878–881
46. Bar-Sagi, D., and Feramisco, J. R. (1985) Microinjection of the ras oncogene protein into PC12 cells induces morphological differentiation. *Cell* **42,** 841–848

47. Willard, F. S., Willard, M. D., Kimple, A. J., Soundararajan, M., Oestreich, E. A., Li, X., Sowa, N. A., Kimple, R. J., Doyle, D. A., Der, C. J., Zylka, M. J., Snider, W. D., and Siderovski, D. P. (2009) Regulator of G-protein signaling 14 (RGS14) is a selective H-Ras effector. *PLos One* **4,** e4884
48. Cao, C., Huang, X., Han, Y., Wan, Y., Birnbaumer, L., Feng, G.-S., Marshall, J., Jiang, M., and Chu, W.-M. (2009) Gα$_{i1}$ and Gα$_{i3}$ are required for epidermal growth factor-mediated activation of the Akt-mTORC1 pathway. *Sci. Signal.* **2,** ra17
49. Rakhit, S., Pyne, S., and Pyne, N. J. (2000) The platelet-derived growth factor receptor stimulation of p42/p44 mitogen-activated protein kinase in airway smooth muscle involves a G-protein-mediated tyrosine phosphorylation of Gab1. *Mol. Pharmacol.* **58,** 413–420
50. Du, Q., and Macara, I. G. (2004) Mammalian Pins is a conformational switch that links NuMA to heterotrimeric G proteins. *Cell* **119,** 503–516
51. Hollinger, S., Ramineni, S., and Hepler J. R. (2003) Phosphorylation of RGS14 by Protein Kinase A potentiates its activity toward Gα$_i$. *Biochemistry* **42,** 811–819
52. Shields, J. M., Pruitt, K., McFall, A., Shaub, A., and Der, C. J. (2000) Understanding Ras. "It ain't over 'til it's over." *Trends Cell Biol.* **10,** 147–154
53. Cho, H., Kim, D.-U., and Kehrl, J. H. (2005) RGS14 is a centrosomal and nuclear cytoplasmic shuttling protein that traffics to promyelocytic leukemia nuclear bodies following heat shock. *J. Biol. Chem.* **280,** 805–814
54. Engert, F., and Bonhoeffer, T. (1999) Dendritic spine changes associated with hippocampal long-term synaptic plasticity. *Nature* **399,** 66–70
55. Manabe, T., Aiba, A., Yamada, A., Ichise, T., Sakagami, H., Kondo, H., and Katsuki, M. (2000) Regulation of long-term potentiation by H-Ras through NMDA receptor phosphorylation. *J. Neurosci.* **20,** 2504–2511
56. Pineda, V. V., Athos, J. I., Wang, H., Celver, J., Ippolito, D., Boulay, G., Birnbaumer, L., and Storm, D. R. (2004) Removal of Gi*α*1 constraints on adenylyl cyclase in the hippocampus enhances LTP and impairs memory formation. *Neuron* **41,** 153–163
57. Tõnissoo, T., Kõks, S., Meier, R., Raud, S., Plaas, M., Vasar, E., and Karis, A. (2006) Heterozygous mice with Ric-8 mutation exhibit impaired spatial memory and decreased anxiety. *Behav. Brain Res.* **167,** 42–48
58. Tõnissoo, T., Meier, R., Talts, K., Plaas, M., and Karis, A. (2003) Expression of ric-8 (synembryn) gene in the nervous system of developing and adult mouse. *Gene Expr. Patterns* **3,** 591–594
59. Zhu, J. J., Qin, Y., Zhao, M., Van Aelst, L., and Malinow, R. (2002) Ras and Rap control AMPA receptor trafficking during synaptic plasticity. *Cell* **110,** 443–455